

Conductivity oscillations in current-induced metastable states in low-doped manganite single crystals

V. Dikovskiy, Y. Yuzhelevskiy, V. Markovich, G. Gorodetsky, and G. Jung*

Department of Physics, Ben Gurion University of the Negev, P.O. Box 653, 84105 Beer-Sheva, Israel

D. A. Shulyatev and Ya. M. Mukovskii

Moscow State Steel and Alloys Institute, 117936, Moscow, Russia

(Received 17 September 2001; revised manuscript received 11 February 2002; published 3 April 2002)

Deterministic oscillations of current-induced metastable resistivity in changing voltage have been detected in $\text{La}_{0.82}\text{Ca}_{0.18}\text{MnO}_3$ single crystals. At low temperatures, below the Curie point, application of specific bias procedures switches the crystal into a metastable resistivity state characterized by the appearance of pronounced reproducible and random structures in the voltage dependence of the differential conductivity. In a certain bias range equally spaced broad conductivity peaks have been observed. The oscillating conductivity has been tentatively ascribed to resonances in a quantum well within the double-tunnel barrier of intrinsic weak links associated with twinlike defect boundaries.

DOI: 10.1103/PhysRevB.65.144439

PACS number(s): 75.30.Vn, 75.25.+z, 73.40.Gk

The transport properties of perovskite manganites are strongly influenced by external factors such as magnetic field, electric fields, hydrostatic pressure, electromagnetic irradiation, and transport current.¹ Spectacular manifestations of electric current effects in perovskite manganites are abrupt, several-orders-of-magnitude-strong, current-enforced resistivity jumps.² The phenomena of resistivity switching in low-doped $\text{La}_{1-x}\text{Ca}_x\text{MnO}_3$ (LCMO) crystals at low temperatures can be seen as a hallmark of transitions into current-induced metastable resistivity states.³ The properties of metastable states depend primarily on the bias history of the sample. Metastable states are characterized by the appearance of reproducible and random structures in the bias dependence of the differential conductivity. The conductivity has a pronounced random noise component, frequently of a non-Gaussian character.⁴ In this paper we report on deterministic periodic conductivity oscillations appearing in current-induced metastable state of $\text{La}_{0.82}\text{Ca}_{0.18}\text{MnO}_3$ single crystal in zero applied magnetic field.

Single crystals of $\text{La}_{0.82}\text{Ca}_{0.18}\text{MnO}_3$ were grown by the floating zone technique, as described in detail elsewhere.⁵ For transport measurements the as-grown sample has been cut into $8 \times 3 \times 1.6 \text{ mm}^3$ rectangular bars with the longest dimension parallel to $\langle 110 \rangle$ crystalline direction. The differential resistance of the sample $R_d = dV/dI$ has been measured using a lock-in technique in a four-point contact arrangement.

Current bias procedures that were employed to create metastable resistivity states in our sample are illustrated in Fig. 1. The LCMO crystal is initially cooled to low temperatures well below the Curie temperature T_c in zero applied magnetic field. Application of the bias current at this stage traces smooth, bell-shaped $R_d(I)$ characteristics shown with a dashed line. The characteristics are fully reversible, provided the bias current does not exceed some thresholds labeled (2) and (3). When the applied current exceeds a threshold value the resistance abruptly drops and the metastable resistivity state (MRS) is established. Upon a subsequent

current decrease to zero followed by an increase towards the negative threshold the distorted-bell-like characteristics of the MRS are traced (dash-dotted line). The MRS $R_d(I)$ characteristics are fully reproducible provided the current does not exceed any of the threshold points. The shape of the MRS characteristics is very close to the one of the pristine state (dashed line); nevertheless, the MRS bell is slightly distorted and contains clearly visible structures, in particular at currents close to the thresholds. When the bias current applied in a direction opposite to that which triggered the preceding transition to the MRS exceeds the threshold value, in the case illustrated in Fig. 1 the threshold (3), sample resistance jumps more pronouncedly and a new metastable low-resistivity state (LRS) is established. The resistance of the LRS (solid line in Fig. 1), is markedly different from previously observed pristine and MRS characteristics. Instead of a bell-shaped form we have a complex curve containing a rich peak structure, pronounced broad minimum at

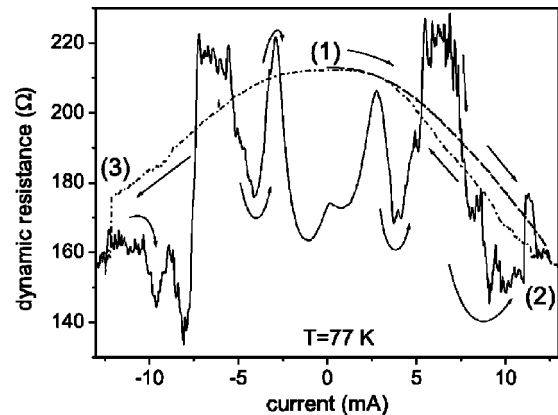


FIG. 1. Current procedures and resulting metastable resistivity states. Current is first increased from (1) (dashed line = pristine state) slightly above the threshold (2), decreased towards zero, and further increased in the negative direction (dash-dotted line = MRS) slightly above the threshold (3). The solid line: subsequent current sweep (LRS) from (3) towards (2).

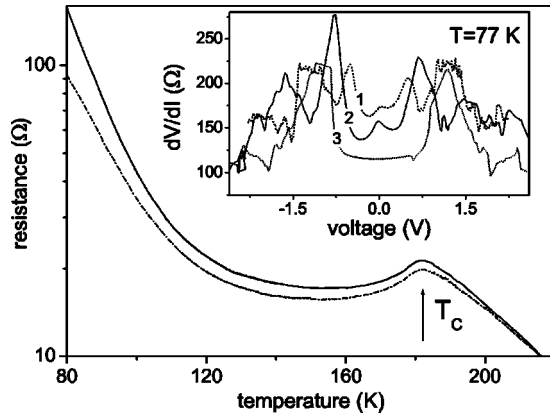


FIG. 2. Temperature dependence of the zero-bias dynamic resistance during a slow warm-up procedure. Solid line: the pristine state. Dash-dotted line: the VLRS state. Area between the lines contains all possible metastable states. Inset: characteristics 1–3 illustrate evolution of the metastable low-resistivity state with increasing range of the bipolar current sweep.

low bias, and a zero-bias anomaly in the form of a small local resistivity maximum at zero bias. The preceding MRS state can be restored by driving the bias current in the positive direction above the threshold (2). Otherwise, for all currents contained between (1) and (2) the sample remains in the LRS. For a current ramp exceeding both thresholds a strong hysteretic behavior is observed. The resistivity seen at the positive-to-negative current direction follows the MRS characteristics, while the LRS characteristics are being traced upon current return from the negative to positive direction.

Obviously, Fig. 1 illustrates just one example of many possible realizations of the metastable resistivity in our sample. Upon increasing the range of the current excursions above the threshold points (2) and (3), the LRS gradually evolves. The zero-bias resistance decreases and conductivity maxima move towards higher voltages. Eventually, upon reaching a certain high-bias threshold the resistance abruptly jumps again and one more metastable state referred to as a very-low-resistivity state (VLRS) is established. The general features of the LRS characteristics are preserved in the VLRS, in particular the resistivity minimum at zero bias and pronounced conductivity peaks. The VLRS is relatively stable and possesses a long-term memory of its resistivity. The memory survives even the thermal cycling to room temperature and maintaining the sample for a few days at 300 K.³

Figure 2 shows the temperature evolution of the pristine and VLRS resistance during a slow warm-up from 77 K to room temperature. The solid line was measured with a sample maintained previously only in the pristine state. The arrow indicates the Curie temperature established from independent magnetization measurements. The Curie point coincides with the local resistance maximum and no significant hysteresis is observed between the cooling and heating runs. The dash-dotted line represents the resistance of a sample in which the VLRS has been enforced by current procedures at 77 K. The VLRS constitutes the lower limit of the observable evolution of the metastable resistivity and thus the area con-

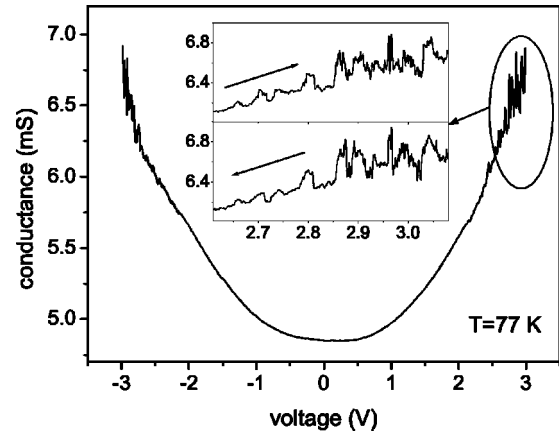


FIG. 3. Conductivity vs voltage in the MRS with pronounced oscillations at bias close to the threshold. The encircled part of the characteristics is shown in the inset for increasing and decreasing current ramps.

tained between solid and dot-dashed lines in Fig. 2 represents the range of available metastable resistivity. The evolution of $R_d(V)$ characteristics with increasing range of the current sweep is illustrated in the inset to Fig. 2. Note that the resistance of all metastable states starts to converge slightly above T_c at a temperature which can be associated with the Jahn-Teller transition.^{3,6}

Metastable resistivity states are characterized by stochastically fluctuating conductivity.⁴ However, we have found that the peak structure associated with the broad zero-bias conductivity maximum remains very reproducible, in particular when plotted as a function of bias voltage rather than current. We have previously suggested that the $R_d(V)$ structures can be associated with the tunnel character of the low-temperature conductivity.³ The tunnel mechanism starts to dominate when the metallic ferromagnetic percolation path becomes more and more interrupted by intrinsic tunnel weak links. The peak structure likely reflects the shape of the density of states in the ferromagnetic areas coupled by the tunnel barrier, or in the barrier itself, as will be discussed elsewhere. In this paper we concentrate on the phenomena of deterministic conductivity oscillations found in the voltage dependence of the dynamic resistivity in a metastable state.

Figure 3 illustrates the voltage dependence of the conductivity of current-enforced MRS. At a bias close to the thresholds the conductivity has a “noisy” character. However, an enlarged view of the encircled part of the characteristics (see inset) shows that the noise constitutes in fact a series of equally spaced peaks. The peak structure is highly reproducible as demonstrated in Fig. 3 by the coincidence of the peak positions in two records measured separately under an increasing and decreasing current. The peak voltages determined for the negative and positive branches of $R_d(V)$ characteristics are plotted in Fig. 4 as a function of the peak number. The data in both directions are well fitted by the linear dependence with the same slope. A good linear fit proves that the observed oscillations are indeed periodic. From the slope of the linear fit we determine that the voltage periodicity of the conductivity oscillations in the MRS is $\Delta V = 39 \pm 1$ mV. The deterministic and periodic nature of

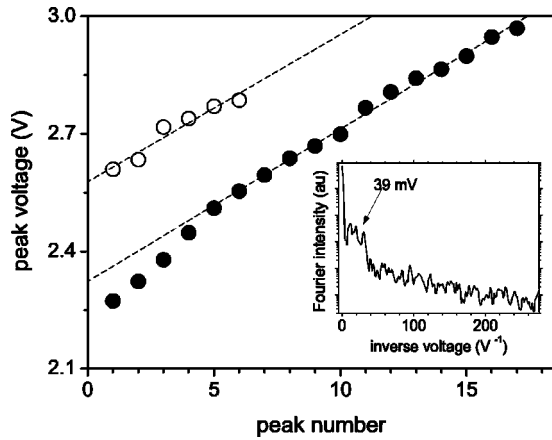


FIG. 4. Voltage positions of the conductivity peaks as a function of the peak number. Solid symbols: positive current. Open symbols: negative current. Inset: averaged Fourier spectrum of several conductivity vs voltage records. The broad peak centered at the voltage periodicity as determined from the peak analysis is indicated by an arrow.

the peak structure has been confirmed by a Fourier analysis. The Fourier spectrum shown in the inset was obtained by averaging several $R_d(V)$ recordings obtained during subsequent current sweeps. The spectrum exhibits a broad peak centered at the voltage corresponding to the period determined by fitting procedures.

At low temperatures, below the metal-insulator transition the phase-separated state becomes the stable ground state of the low-doped LCMO compound and the ferromagnetic phase forms percolating conducting paths. With decreasing temperature the volume of the ferromagnetic phase increases. However, as indicated by the resistivity upturn in Fig. 2 and by the nonlinear character of the I - V characteristics, the low-temperature conductivity is dominated by a tunnel mechanism. Although absolute proof of tunnel conductivity cannot be provided, we remind the reader that we have previously shown that the voltage and temperature dependences of the resistance can be very well fitted to the Glasman-Matveev (GM) model of indirect tunneling.^{3,7} The nature of the involved intrinsic tunnel junctions remains still an open question. Growth of the insulating phase that interrupts the percolation path at low temperatures is one of the possible scenarios. Nevertheless, in the existing literature there is no consensus about the existence of the low-temperature phase transition to the insulating state at the doping range of our samples.¹ On the other hand, using the magneto-optic (MO) techniques we have always detected in our crystal at temperatures below T_c a regular pattern of stripelike domains with an alternating level of magnetization. The MO contrast of the stripes depends on the applied field, and the high and low magnetization inverts coherently upon inverting the field direction, but neither the strip positions nor their size, in the range of 50–200 μm , do not change with changing field and temperature. On subsequent cooling cycles the details of the pattern change but the overall features remain invariant. This indicates the structural origin of the magnetic patterns.

The most probable source of stripe-shaped domains can be the occurrence of twins, rotation defects, or regular grain boundaries in the investigated crystal. Manganite colossal magnetoresistance (CMR) crystals are known to contain twinlike structural defects which are strongly correlated with magnetic domains.^{8–10} Moreover, in low-doped LCMO such defects are capable of pinning and preventing the motion of the magnetic domain walls.¹¹ We note at this point that the observed MO domain size and direction within the crystal are not constant. The domain structure does not reflect, therefore, the presence of coherent twins similar to those in manganites with charge-ordered low-temperature phase transition.¹² This is due to the absence of an intrinsic martensitic transition in a 0.18 LCMO system. Intrinsic tunnel weak links in low-carrier-density manganites are prone to be localized at structural defects. Band bending effects in the ferromagnetic metallic phase in the vicinity of a twin or grain boundary result in the creation of depletion layers acting as localized insulating tunnel barriers.^{13,14} The band bending and, consequently, the intrinsic junction conductance depend on the difference in magnetization between adjacent domains. Due to the stress associated with the lattice mismatch, a few nm thick strongly disordered accommodation layer containing arrays of dislocations is formed within the boundary.¹³ The stress field within the accommodation layer results in a local depression of the Curie temperature and the creation of an interfacial conducting layer contained between two insulating tunnel barriers on both sides of the twin boundary.^{13,14} Consequently, the intrinsic junction has the complex structure of a double-barrier tunnel junction.

It has been shown theoretically and confirmed experimentally that a nonmagnetic interface layer, even within a single-tunnel barrier magnetic junction, behaves as quantum well leading to resonant enhancements of conductivity whenever a resonant condition for a quantum well state is fulfilled.¹⁵ In a double-barrier magnetic tunnel junction, quantum well layer resonances enable coherent tunneling of electrons through the entire junction resulting in strong enhancement of the conductivity at resonant conditions.^{16,17} In the approximation of the spin-polarized free electron model the quantum well resonances occur whenever $k_F a = n\pi$, where a is the width of the interface layer and k_F the Fermi wave vector.^{16,18} This model predicts that the periodicity of conductivity oscillations is

$$\Delta V \approx \frac{h}{4a^2 m} \frac{h}{2e}. \quad (1)$$

By confronting the experimentally determined periodicity of conductivity oscillations with the prediction of the model we obtain the width of the interface disordered layer $a = 3.1$ nm.

Let us point out that a regular network of grain boundaries can by itself lead to resonances in a multibarrier spin-dependent system of ferromagnetic quantum wells.¹⁸ This scenario is, however, very unlikely due to the macroscopic distances between the twin boundaries seen in the magneto-optics images. Scattering processes during electron transit between individual boundaries will prevent the formation of

quantum well states. Another alternative mechanism for conductivity oscillations assumes the existence of a small mesoscopic metallic grain within the tunnel barrier. If the grain is small enough, the charging effect may lead to Coulomb blockade of the tunneling current.¹⁹ However, estimations of the grain size and resulting periodicity at 77 K give unrealistic values, far from those observed in the experiments, while estimations based on the double-barrier grain boundary

junction give very plausible values for the disordered interface layer thickness. Therefore, despite the fact that we cannot provide direct proof of the validity of the proposed mechanism, we believe that coherent spin-polarized resonant tunneling lies behind the experimentally observed conductivity oscillations.

This research was supported by Grant No. 209/01 from Israeli Science Foundation.

*Also with Institute of Physics, PAN, 02-668 Warszawa, Poland.

¹E. Dagotto, T. Hotta, and A. Moreo, *Phys. Rep.* **344**, 1 (2001).

²A. Asamitsu, Y. Tomioka, H. Kuwahara, and Y. Tokura, *Nature (London)* **388**, 50 (1997); J. Stankiewicz, J. Sese, J. Garcia, J. Blasco, and C. Rillo, *Phys. Rev. B* **61**, 11 236 (2000); S. Srivastava, N. K. Pandey, P. Padhan, and R. C. Budhani, *ibid.* **62**, 13 868 (2000).

³Y. Yuzhelevski, V. Markovich, V. Dikovskiy, E. Rozenberg, G. Gorodetsky, G. Jung, D. A. Shulyatev, and Ya. M. Mukovskii, *Phys. Rev. B* **64**, 224428 (2001).

⁴Y. Yuzhelevski, V. Dikovskiy, V. Markovich, G. Gorodetsky, G. Jung, D. Shulyatev, and Ya. M. Mukovskii, *Fluct. Noise Lett.* **1**, L105 (2001).

⁵D. A. Shulyatev, A. A. Arsenov, S. G. Karabashev, and Ya. M. Mukovskii, *J. Cryst. Growth* **188/189**, 511 (1999).

⁶G. Biotteau, M. Hennion, F. Moussa, J. Rodriguez-Carvajal, L. Pinsard, A. Revcolevschi, Y. M. Mukovskii, and D. Shulyatev, *Phys. Rev. B* **64**, 104 421 (2001).

⁷L. I. Glasman and K. A. Matveev, *Sov. Phys. JETP* **67**, 1276 (1988).

⁸B. B. van Aken, A. Meetsma, and T. T. M. Palstra, *cond-mat/0103628* (unpublished).

⁹A. Khapikov, L. Uspienskaya, I. Bdikin, Ya. Mukovski, S. Karabashev, D. Shulayev, and A. Arsenov, *Appl. Phys. Lett.* **77**, 2376 (2000); V. K. Vlasko-Vlasov, Y. K. Lin, U. Welp, G. W. Crabtree, D. J. Miller, and V. I. Nikitenko, *J. Appl. Phys.* **87**, 5828 (2000).

¹⁰V. K. Vlasko-Vlasov, Y. K. Lin, D. J. Miller, U. Welp, G. W. Crabtree, and V. I. Nikitenko, *Phys. Rev. Lett.* **84**, 2239 (2000).

¹¹M. Pissas, G. Kallias, M. Hofmann, and D. M. Töbrens, *Phys. Rev. B* **65**, 064413 (2002).

¹²V. Podzorov, B. G. Kim, V. Kiryukhin, M. E. Gershenson, and S.-W. Cheong, *Phys. Rev. B* **64**, 140406(R) (2001).

¹³R. Gross, L. Alff, B. Büchner, B. H. Freitag, C. Höfner, J. Klein, Yafeng Lu, W. Mader, J. B. Philip, M. R. S. Rao, P. Reutler, S. Ritter, S. Thienhaus, S. Uhlenbruck, and B. Wiedenhorst, *J. Magn. Magn. Mater.* **211**, 150 (2000), and references therein.

¹⁴C. Höfner, J. B. Philipp, J. Klein, L. Alff, A. Marx, B. Büchner, and R. Gross, *Europhys. Lett.* **50**, 681 (2000).

¹⁵W.-S. Zhang, B.-Z. Li, and Y. Li, *Phys. Rev. B* **58**, 14 959 (1998); J. S. Moodera, J. Nowak, L. R. Kinder, P. M. Tedrow, R. J. M. van de Veerdonk, B. A. Smits, M. van Kampen, H. J. M. Swagten, and W. J. M. de Jonge, *Phys. Rev. Lett.* **83**, 3029 (1999); W.-S. Zhang, B.-Z. Li, X. Zhang, and Y. Li, *J. Appl. Phys.* **83**, 5332 (1998).

¹⁶Z. Zheng, Y. Qi, Y. Xing, and J. Dong, *Phys. Rev. B* **59**, 14 505 (1999).

¹⁷M. Wilczynski and J. Barnas, *J. Magn. Magn. Mater.* **221**, 373 (2000); *Sens. Actuators A* **91**, 188 (2001).

¹⁸X. Zhang, B.-Z. Li, G. Sun, and F.-C. Pu, *Phys. Rev. B* **56**, 5484 (1997); A. Vedyayev, N. Rizhanova, B. Vlutters, B. Dienen, and N. Strelkov, *J. Phys.: Condens. Matter* **12**, 1797 (2000).

¹⁹K. Nakajima, Y. Saito, S. Nakamura, and K. Inomata, *IEEE Trans. Magn.* **36**, 2806 (2000).